Journal of Applied Mathematics and Physics, 2017, 5, 1763-1775
http://www.scirp.org/journal/jamp
ISSN Online: 2327-4379
ISSN Print: 2327-4352

Conceptual Design of Beam Tube of 300 KeV Electron Electrostatic Accelerator

Seied Isa Karanian[1], Ramin Roozehdar Mogaddam[1*], Elnaz Seifnouri[2], Mehdi Amiri[3]

[1]Faculty of Science, Emam Ali University, Tehran, Iran
[2]Physics Department, Islamic Azad University, Karaj Branch, Iran
[3]Department of Physics, University of Mohaghegh Ardabili, Ardabil, Iran
Email: seiedisa.karanian@gmail.com, *ramin.roozehdarmogaddam@stu.um.ac.ir

How to cite this paper: Karanian, S.I., Mogaddam, R.R., Seifnouri, E. and Amiri, M. (2017) Conceptual Design of Beam Tube of 300 KeV Electron Electrostatic Accelerator. *Journal of Applied Mathematics and Physics*, **5**, 1763-1775.
https://doi.org/10.4236/jamp.2017.59149

Received: May 2, 2017
Accepted: September 18, 2017
Published: September 22, 2017

Abstract

The column of electron electrostatic accelerator is one of the critical components in electrostatic accelerator. The geometrical design of such accelerator must be as such that in the case of applying voltage to its electrodes, not only should its equipotential surfaces and its gradient accelerate the beam particles up to desired energy, but also it should focus the beam and hinder broadening of energy distribution of accelerated particles. The immersed electrodes in the field are, geometrically, perpendicular to optical axis around the medial plane. Numerous models that can be used in the distribution of axial potential, have been presented and linear model, analytical model, double-column electrode model and polynomial electrode model are among them. In this paper, series expansions based on Bessel functions is used to obtain the axial potential distribution of immersed accelerator electrodes in double-electrode field and it is then compared to the mentioned models by solving the final equation via the least square method. Finally, by using CST Studio software and the information we obtained from the axial potential, the column of electron accelerator with its energy distribution and its optimal electron output beam radius is designed and simulated.

Keywords

Accelerator Tube, Lenses Immersed in the Field, Axial Potential Distribution, Electrode

1. Introduction

Application of accelerator is common in many fields such as research, education, industry, medicine [1] and agriculture. The aim of designing the column of an accelerator is to accelerate electrons to energies more than 300 KeV by using electrostatic field. Electrostatic accelerators are regarded as the simplest and yet frequently-used accelerators. Depending on the energy and the generated beam, these accelerators can find many applications [2]. One of the important topics pertinent to the physics of accelerators is the electrostatic lenses; since they can be implemented in construction of accelerator's tube in accelerators. After many years of research in laboratories regarding the design, construction and completion of accelerator's tube, this part is still regarded as one of the key components in construction of electrostatic accelerators [3]. Electrostatic electrodes are mainly used for constructing an image in a fixed position with broad range of beam energy [4] [5]. The electrostatic electrodes are widely categorized in terms of the potential of their electrodes (image potential over object potential) which contain the main group of Einzel lens [6] [7] [8], which create similar potential in both object part and image part, the immersed lens in the field are immersed in a field with two constant but different potentials in the both sides, a single-span lens with one induced homogeneous field on one side, and the foiled lens [9]. In case of unequal potentials in both sides of the lens, the lens operates in accelerator or decelerator (velocity reducer) mode. All of the lenses presented above can contain two or more electrodes [10] [11]. Double-electrode lenses are generally used in focusing the electron or proton beams [9].

In addition to identifying electrostatic lenses with their electrodes, they can also be verified by their axial potential distribution; this is due to the fact that majority of the focusing elements which have axial symmetry in ion optics or electron optics can be denoted by a scalar potential function [5]. General operation of electrostatic lenses is in a way that by creating an axially symmetric potential, a paraxial beam is generated which its radial growth can be impeded when directed to target. The equation below can be used to calculate the particle trajectory in an electrostatic lens in non-relativistic terms and without a magnetic field:

$$\frac{\mathrm{d}^2\sigma}{\mathrm{d}z^2}+\frac{3}{16}\left[\frac{U'(z)}{U(z)}\right]^2\sigma=0 \tag{1}$$

which $U(z)$ and $U'(z)$ are axial potential and field, respectively. σ denotes the path of particles [12] [13]. The simplest kind of electrostatic lens has two electrodes in which if potential in the two sides differ, then it is called immersed in field. Extensive changes of parameters of electrodes cannot be verified practically and systematically. Therefore, we commence with the analysis of potential distribution. The figure of axial potential distribution $U(z)$ of an electrode in two-piece field is approximately similar to that of an tangent hyperbolic function, which is a steady function of z coordinate. Let the potential of the first and second electrodes be V_1 in $z=a$ and V_2 in $z=b$, respectively. When $|V_2|>|V_1|$ an accelerator lens is formed while as when $|V_2|<|V_1|$ a decelerator lens will be formed. In these lenses, potential distribution will not include the region with constant potential since to preserve these regions more electrodes are required [3] [12].

2. Numerical Calculation of Axial Potential of the Immersed Lens in Field with Bessel Function Expansion Series

In order to calculate the axial potential of a lens immersed in field, we consider two flat planes which each of them have holes in them with the diameter of D and they are separated from each other with distance A. The applied voltages to these planes (electrodes) are V_1 and V_2 which have been calculated relative to potential of electrons with zero kinetic energy. In the upcoming equations the thickness of planes have been neglected (if the thickness is smaller than A and D, the dependence of lens parameters to thickness will be negligible). It is also required to consider three hypothetical cylinders with diameter D' which cylinders in regions I and III have potential V_1 and V_2 whereas the middle cylinder possess the linear potential running from V_1 to V_2 in its length.

It might be argued that having the middle cylinder in a uniform potential V_m (which, for instance, is equal to V_1 or V_2 or their average) is more in accordance with real lenses; however this is not the case for two reasons: firstly, if $D' \lesssim 2A$, then such middle cylinder will alter the axial potential distribution between the holes and it would be necessary to calculate the lens parameters for different values of D' and V_m; secondly, if $D' \gtrsim 2A$, the lens parameters would partly be analogous to the case in which the potential of middle cylinder is changing linearly, but the calculations will get longer and the accuracy will deplete.

Figure 1 exhibits the paraxial and non-paraxial beams alongside the object distance P and image distance Q, which both have been measured in regard with the central point of the lens. In calculations of electrostatic lenses with digital computers, the common way is to solve the Laplace equation [14]. There is another solution approach in which the potential is expanded by Bessel functions.

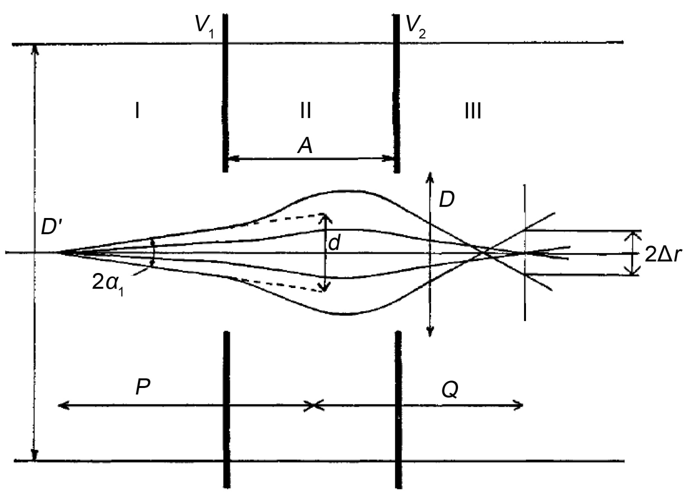

Figure 1. Geometry of investigated lenses.

Despite the fact that solution procedure of Laplace equation is a familiar simplification method, more precise and reliable results can be obtained faster with high degree of accuracy by modification of its expansion. It seems that the method used in these calculations will serve more precisely and strongly for wide range of problems with cylindrical symmetry. The series expansion for the three regions in **Figure 1** can be written as follows [15]:

$$V_{\mathrm{I}}(r,z) = V_1 + \sum_n A_n \exp(k_n z) J_0(k_n r) \tag{2}$$

$$V_{\mathrm{II}}(r,z) = \frac{V_1+V_2}{2} + \frac{V_2-V_1}{A} z + \sum_n \left\{ B_n \exp(-k_n z) + B'_n \exp(k_n z) \right\} J_0(k_n r) \tag{3}$$

$$V_{\mathrm{III}}(r,z) = V_2 + \sum_n C_n \exp(-k_n z) J_0(k_n r) \tag{4}$$

Which the equations above are written in cylindrical coordinate and z is measured form central point of the lens. $J_0(x)$ is the zero order Bessel function. Each term of these expansions is a solution of Laplace equation with no boundary conditions. The signs which are associated to exponential variables are chosen in a manner that the boundary conditions in $z = \pm\infty$ are automatically satisfied. Boundary condition in $r = \frac{1}{2}D'$ would be fulfilled if the values of K_n become limited which then we obtain:

$$J_0\left(\frac{1}{2}k_n D'\right) = 0 \tag{5}$$

Now the only task that remains is to meet the boundary conditions in $z = \pm\frac{1}{2}A$, in addition we will have to make sure that the potential stays continuous all over the two holes.

From orthogonally condition for Bessel functions and from the condition:

$$V_{\mathrm{I}}\left(r, -\frac{1}{2}z\right) = V_{\mathrm{II}}\left(r, -\frac{1}{2}z\right) \quad \text{for } 0 \le r \le \frac{1}{2}D' \tag{6}$$

the following will result for all values of n:

$$A_n \exp\left(-\frac{1}{2}k_n A\right) = B_n \exp\left(\frac{1}{2}k_n A\right) + B'_n \exp\left(-\frac{1}{2}k_n A\right) \tag{7}$$

This equation will also guarantee that the radial component of the field remain continuous. The boundary condition for the left-hand-side electrode for $\frac{1}{2}D \le r_2 \le \frac{1}{2}D'$ will obviously be [12]:

$$\sum_n \left\{ B_n \exp\left(\frac{1}{2}k_n A\right) + B'_n \exp\left(-\frac{1}{2}k_n A\right) \right\} J_0(k_n r_2) = 0 \tag{8}$$

And for $0 \le r_1 \le \frac{1}{2}D'$ we will have [12]:

$$\sum_n B_n k_n \exp\left(\frac{1}{2}k_n A\right) J_0(k_n r_1) = \frac{V_2 - V_1}{2A} \tag{9}$$

The same is also applied to second hole. Due to the symmetry around central point, equations $B_n' = -B_n$ and $C_n = -A_n$ will be true. Although Equations (8) and (9) are precisely satisfied when infinite number of terms is considered, we can still hope that finite number N of terms, the difference between the right and left side of these equations will rationally approach zero. Thus, N number of R will be selected within 0 to D' and N obtained equation of (8) and (9) will be used to calculate N coefficient of B_n. This process will not converge by increasing N but instead, will lead to. For r values amongst the chosen ones, Equations (8) and (9) will poorly meet.

To overcome this problem many useful methods can be used but the least square method proves to be the most effective one and thus was used. In our problem, the least square method will contain forming the quantity.

$$S = \sum_{r_2}\left[\sum_{n=1}^{N} B_n \left\{\exp\left(\frac{1}{2}k_n A\right) - \exp\left(-\frac{1}{2}k_n A\right)\right\} J_0\left(k_n r_2\right)\right]^2 + \sum_{r_1}\left\{\sum_{n=1}^{N} B_n k_n \exp\left(\frac{1}{2}k_n A\right) J_0\left(k_n r_1\right) - \frac{V_2 - V_1}{2A}\right\}^2 \tag{10}$$

And then obtaining N equation from $\frac{\partial S}{\partial B_n} = 0$ condition for $1 \le n \le N$:

$$\sum_{r_2}\left[\sum_{j=1}^{N} 2B_j \left\{2\sinh\left(\frac{1}{2}k_j A\right)\right\} J_0\left(k_j r_2\right)\right]\left[\left\{2\sinh\left(\frac{1}{2}k_i A\right)\right\} J_0\left(k_i r_2\right)\right\} + \sum_{r_1} 2\left\{\sum_{j=1}^{N} B_j k_j \exp\left(\frac{1}{2}k_j A\right) J_0\left(k_j r_1\right) - \frac{V_2 - V_1}{2A}\right\} k_i \exp\left(\frac{1}{2}k_i A\right) J_0\left(k_i r_1\right) = 0 \tag{11}$$

Next for calculating B_n coefficients the equation can be solved. By writing a Fortran code, which can be generalized to more electrodes, and selecting $V_1 = 100\ \text{V}$, $V_2 = 60\ \text{V}$, $d = 3\ \text{cm}$ and $N = 20$ unknown coefficients will be attained numerically via the above equations and by substituting them in Equations (1) and (3), the potential will be specified for double-electrode electrostatic lens which is shown in **Figure 2**. Selecting $r = 0$ yields the axial potential distribution.

It should be noted that the values of $r_1\left(0, \frac{1}{2}D\right)$ and $r_2 = \left(\frac{1}{2}D, \frac{1}{2}D'\right)$ must be greater than N (about $3N$ in practice). This will result in converging solutions for Equations (8) and (9) and axial potential $V(0,z)$ which in this case will converge by increasing N.

3. Models for Investigation of Electrostatic Lenses Immersed in Field

In potential distribution of double-electrode systems, there exists a bending point Z_m which its axial component of field $\left(|U'|_{\max}\right)$ reaches to its maximum pure value. This point can be located in either the geometrical center or any other point and this is the reason why those two symmetric lenses can be defined [10]. In case of immersed lenses in field which are geometrically symmetric around the optical axis perpendicular to central plane, *i.e.* position of Z_m is

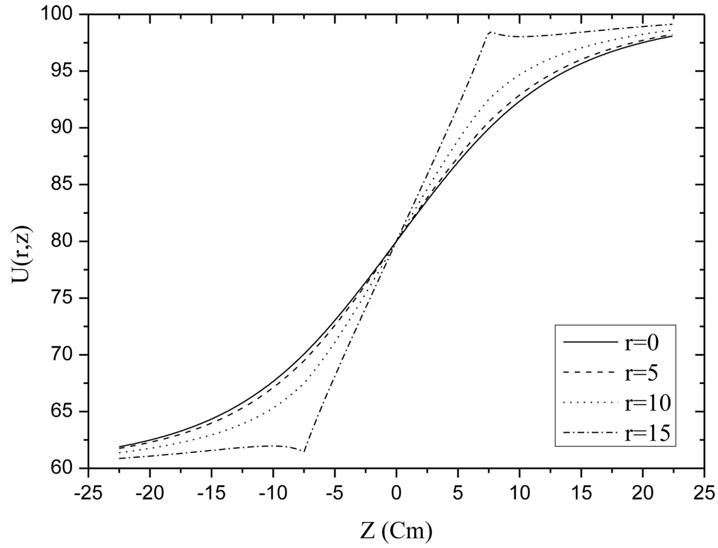

Figure 2. z-dependent potential for constant radius of *r*. Potentials on the electrodes are $V_1 = 100\ \text{V}$ and $V_2 = 60\ \text{V}$.

precisely coincident with the average value of *a* and *b*, some models have been proposed to specify the asymmetric potential distribution around Z_m. Different models have been presented for axial potential distribution of this system which linear model, analytical model, double-cylinder lens model, and polynomial lens model are some to mention. **Figure 3** compares the least square model with the aforementioned methods.

Axial potential distribution for immersed lens in field has been displayed in **Figure 4** for different values of A/D. Numerical calculations reveal that the best state of minimum output beam radius and maximum output energy of aperture lens is for the case in which the diameter of electrodes are identical and the ratio of distance to diameter is between 0.1 to 0.3.

4. Design and Simulation of Column of 300 KeV Accelerator

In order to simulate the column of accelerator, the outer radius of electrodes has taken the value of 15 centimeters; therefore we consider the distance between electrodes to be 5 centimeters so as to have the optimal state for column of the accelerator. The other restrictive factor in choosing the distance between electrodes is formation of arc and electric refraction. The distance between the electrodes can be determined by Equation (12) [9]:

$$V = CX^{\alpha} \tag{12}$$

where V is the potential difference of the two consecutive electrodes, α is a constant value between 0.1 and 1.1 and C is also a constant value which depends on the intensity of the electric field, distance between electrodes and their material. Majority of systems assumes α to be between 0.5 and 0.7. Considering the applied potential to the planes and by obeying the 5 cm-rule between the electrodes, one can avoid electric discharge. Insulators made of borosilicate glass

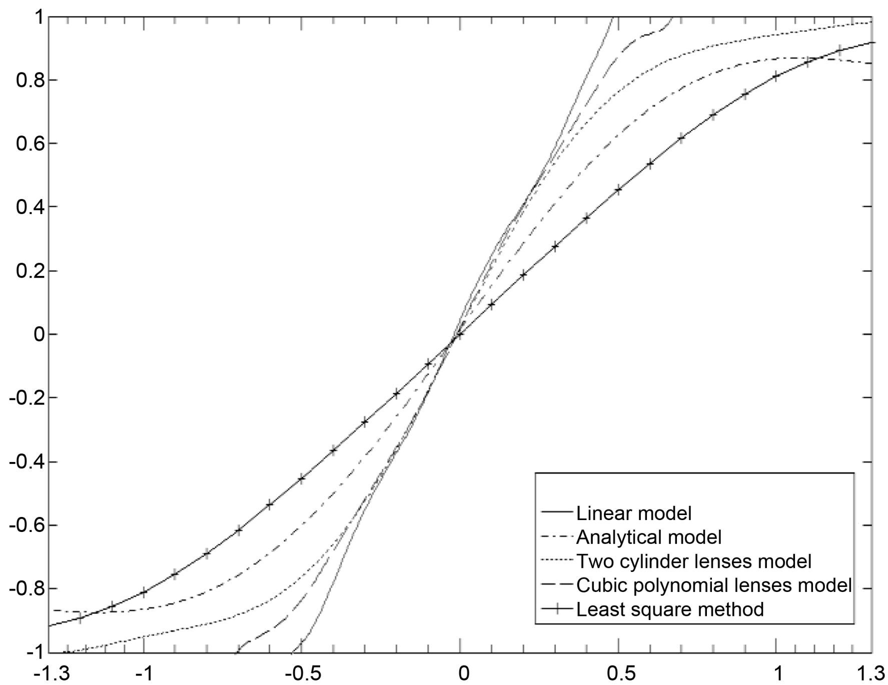

Figure 3. Potential distribution of immersed lens in symmetric binary field: linear model [12], analytical model, two-cylinder lens model with zero distance between the electrodes [16] [17], cubic polynomial lens model [12], least square method.

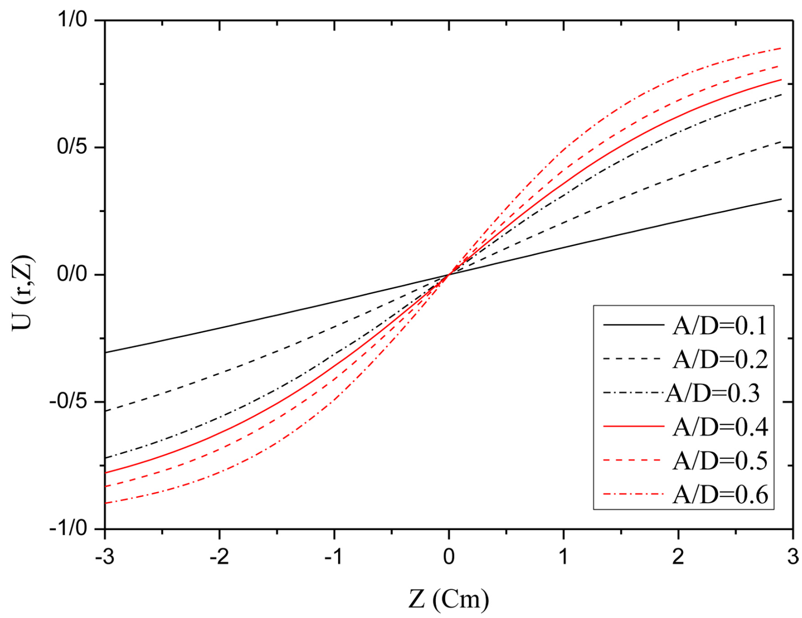

Figure 4. Axial potential distribution of immersed lens in field for different values of A/D.

or electrical ceramics (alumina-based) can be put in between the electrodes of column of accelerator to avoid occurrence of electric discharges. Moreover, they can generate the required vacuum (about 10 - 5 torr in lab) for the column of accelerator.

Simon and Superfish computer codes [16] are normally used in designing the electrodes and simulating the electric field of electrodes of accelerator's column. One of the major problems that almost all of the simulation programs has, is that true definition for vacuum, electric refractions, and interaction of particles with the system chamber cannot be applied. Hence, our attempt was to provide a coding program that firstly has these capabilities and secondly, it can perform Monte Carlo and result a more accurate response. CST software uses Monte Carlo method to draw the beams and display the trajectory of particle. CST has been used for simulation. This software is regarded as one the most powerful software in numerical simulation of electromagnetic fields, design of different antenna, design of electric circuits, and high frequency circuits which is the life-long fruit of research and endeavor in the field of electromagnetic analysis and design. The observations are shown in three dimensions which are requisites in electromagnetic circuits. The design of accelerator column, according to our experience from building the proton accelerator column, has taken the form of **Figure 5**.

Since we want the beam current to be in the order of a few microamperes in this accelerator column, Perveance beam $K = \left(\frac{I}{V^{\frac{3}{2}}} \right)$ is negligible. Therefore, we can disregard the spatial charge effects in designing electrodes. In **Figure 5**, the first electrode from left extracts electrons, the second and forth electrodes focus the beam, third electrode acts as a shield against outer fields and fifth till fourteenth electrodes are accelerating electrodes. The applied potential is divided evenly amongst all electrodes. Potential of −300 kV relative to earth with step potential of 25 kV (choosing this potential is absolutely voluntary and is dependent upon the geometry of the accelerating system, other step potentials can be taken into account) is divided amongst the electrodes, except second electrode;

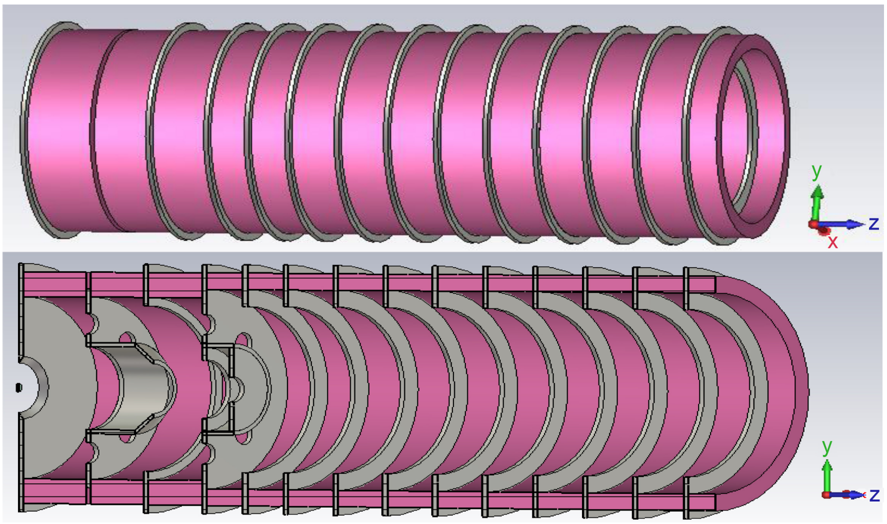

Figure 5. Design of electrostatic accelerator column of electron with accelerating electrodes.

i.e. the first, third, fourth, …, last electrodes will have potentials of −300 kV, −275 kV, −250 kV, …, 0 kV relative to earth, respectively.

The second electrode which acts as the focusing lens of the column has variable voltage of +10 kV relative to the first one. Titanium has the lowest field emission, micro-discharge, arc-driven surface abrasion, best stable voltage, most work function and electric gradient in low distances. Due to these reasons a titanium-based material can be determined in designing electrodes. Nevertheless, the machining and burnishing process of titanium is more costly and burdensome in comparison with other metals. Thus, aluminum is suitable option in designing. The overall number of 14 electrodes will be implemented. For Figure 5, by applying the given potentials, potential distribution and axial potential distribution will result in Figure 6.

Trajectory of particles is shown in Figure 7(a) and Figure 7(b) displays the energy of electrons. Electron beams are once focused in distance of 5 - 10 cm and then again in 20 - 25 cm, which indicates that the focusing electrodes have been designed properly. The output electron beam radius will be less than 8 mm (electrons exit in distance of 72 cm away from the accelerator column) and electron beam energy, at the time of exiting the accelerator column, will be in range of 250 keV.

As it can be seen from Figure 8, if we set the voltage of second electrode to be −300 kV relative to earth, the output electron beam energy will approximately be around 300 keV.

In the second geometry for optimizing of application of accelerator column, the electrodes can be considerated ridged that is shown in Figure 9:

The path of the particles for the second geometry in Figure 10(b) and electron energy in the form of Figure 10(a) is given which shows the radius of output beam in second geometer is reduced 2 cm and the energy of electrons is increased in compare with first geometer; So it is better to design the electrodes of 300 keV electron electrostatic accelerator column ridged.

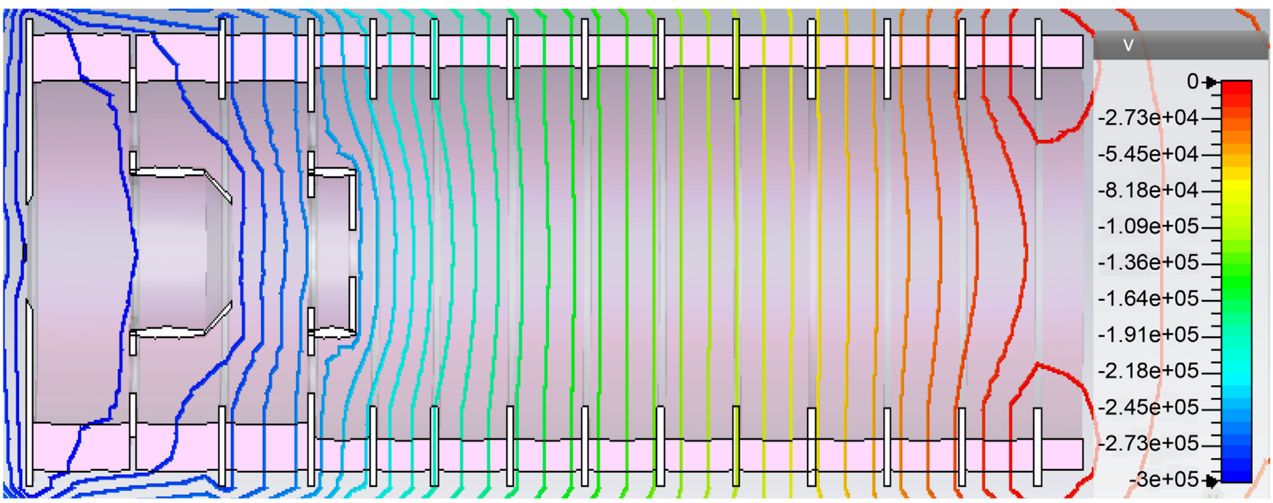

Figure 6. Equipotential lines along the accelerator column.

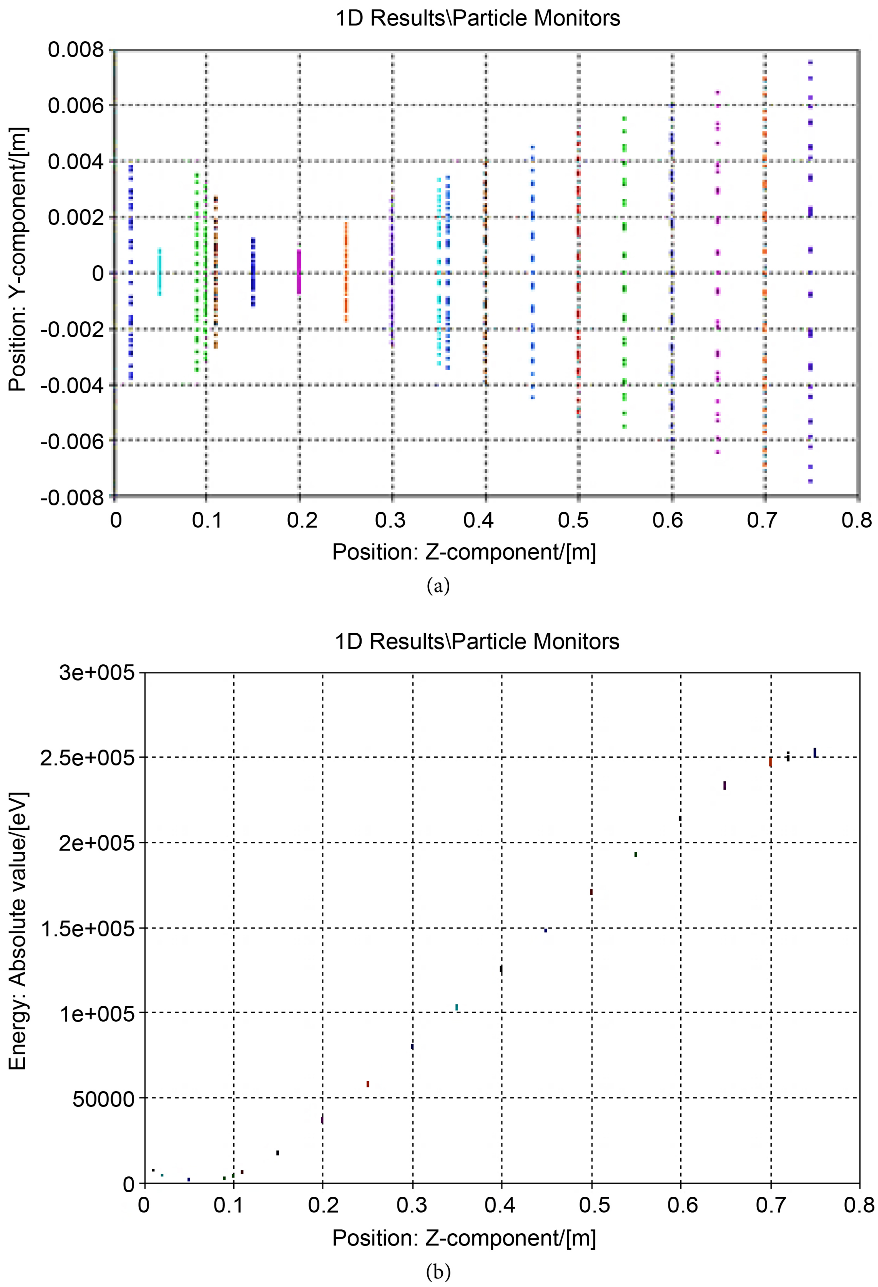

Figure 7. (a) electron beam trajectory (b) electron beam energy while crossing the accelerator tube for $V_2 = -290\ \text{kV}$.

In case of needing an electron beam with radius of lower than 6 mm, an electric quadrupole lens can be located at the exiting direction of electron beam to control the output beam radius. In this software, complete vacuum has been regarded for beam trajectory and since this is not achievable in reality, it would be better to set the total voltage of accelerator column to more than −300 kV.

5. Conclusion

For designing and manufacturing the accelerator tube should have comprehensive

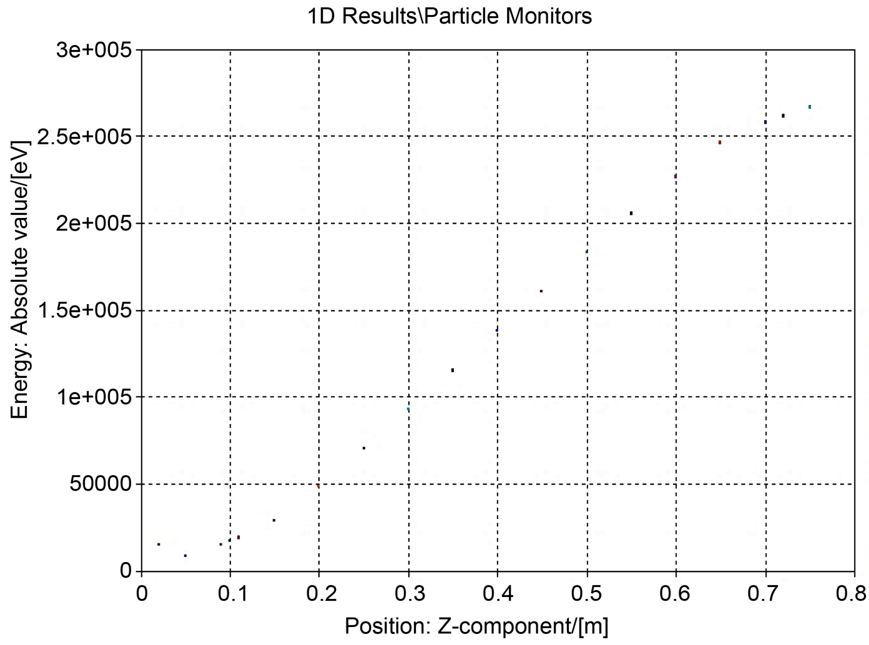

Figure 8. Electron beam energy while crossing the accelerator tube for $V_2 = -300\ \text{kV}$.

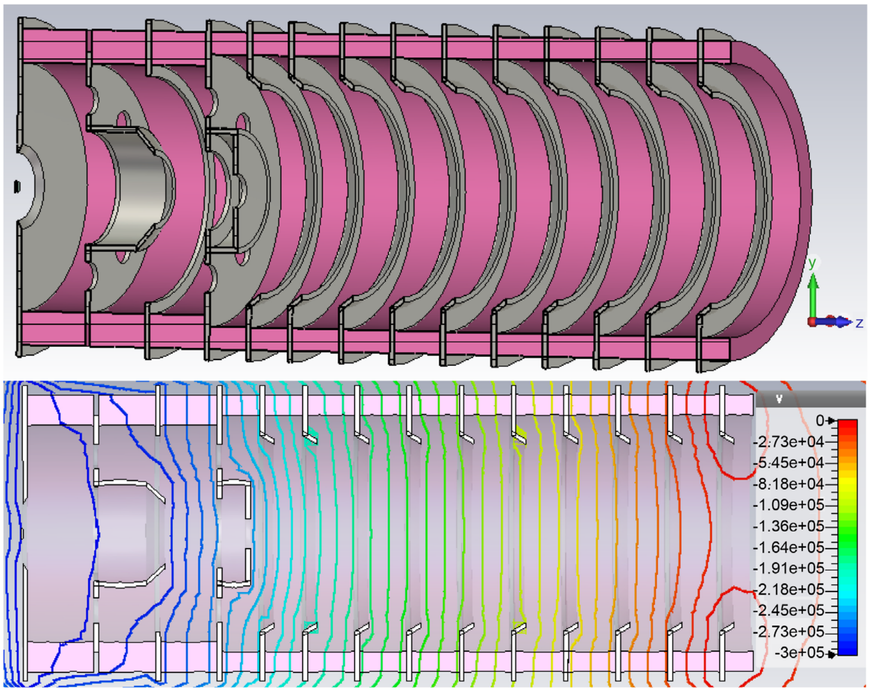

Figure 9. Designing of electrostatic electron accelerator column with ridged accelerator electrodes. this causes some changes in equipotential surfaces and electron beam will be more focal.

information of the electrostatic lenses for electrons, protons and ions under the influence of an electrical potential gradient that these lenses create, will be accelerated and reaches to final desired speed. As well as focusing the beam of charged particles is also the responsibility of these lenses. In the case of controlling

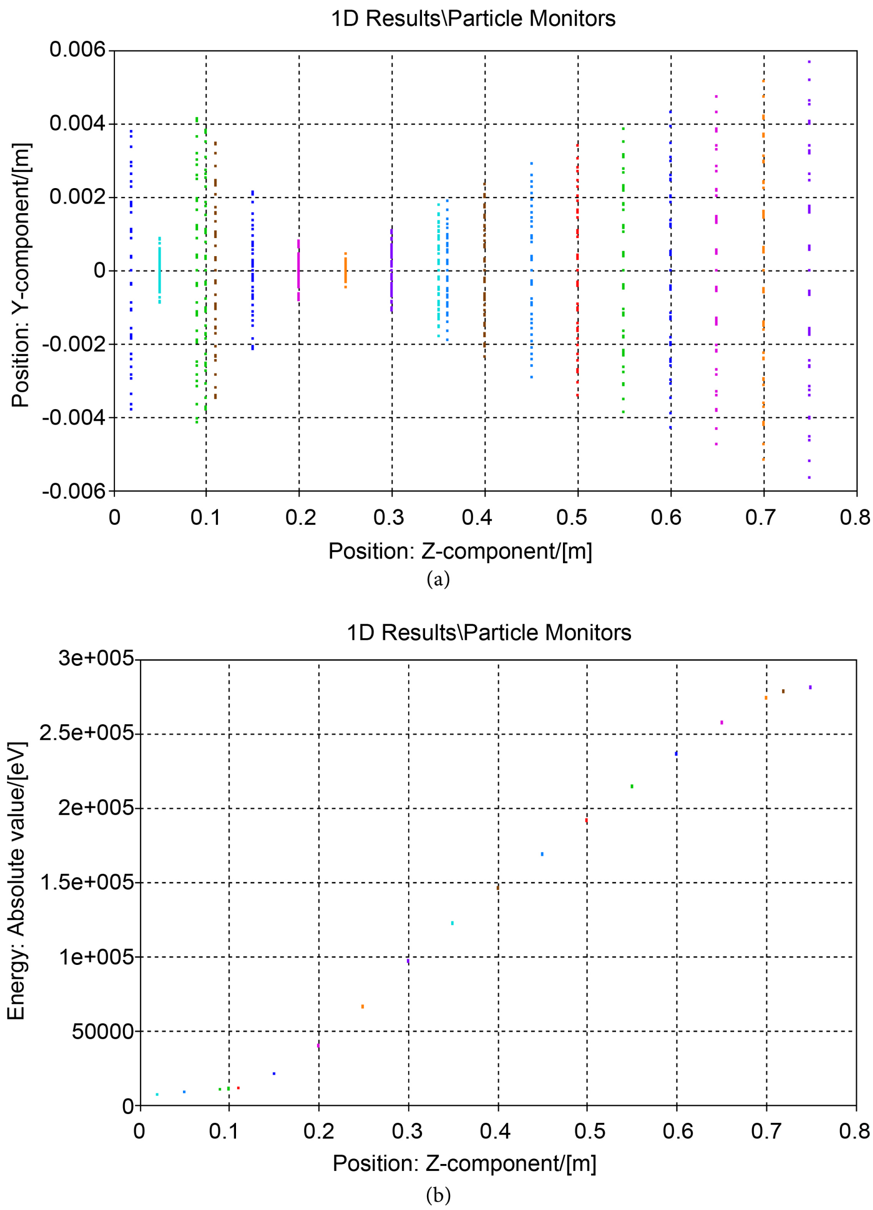

Figure 10. (a) electron beam trajectory (b) electron beam energy for the second geometry of electrodes when $V_2 = -290\ \text{kV}$.

low-energy beam, two electrodes electrostatic lenses are used.

Using an axial potential distribution which can be characterized by an electrostatic lens, can predict how charged particle beams move. Numerical calculations show that the best situation for lens that makes output electron beam energy maximum and focal is when electrodes diameter are the same and the rate of distance between electrodes to diameter is 0.1 to 0.3. First geometry that is designed reaches to 8 mm of output beam diameter and 270 keV of energy but when we use ridged electrodes, diameter of output beam will decrease to 6 mm and energy will increase to 300 keV. Of course it is predictable by comparing equipotential surfaces in **Figure 6** and **Figure 9**.

References

[1] Cartelli, D., Thatar Vento, V., Castell, W., Dipaolo, H., Kesque, J. M., Bergueiro, J., *et al*. (2011) Accelerator Tube Construction and Characterization for Tandem-Electrostatic-Quadrupole for Accelerator Based Boron Neutron Capture Therapy. *Applied Radiation and Isotopes*, **69**, 1680-1683. https://doi.org/10.1016/j.apradiso.2011.01.017

[2] Brown, T.A. and Gillespie, G.H. (2000) Optics Elements for Modeling Electrostatic Lenses and Accelerator Components: III. Electrostatic Deflectors. *Nuclear Instruments and Methods in Physics Research Section B*: *Beam Interactions with Materials and Atoms*, **172**, 338-343. https://doi.org/10.1016/S0168-583X(00)00097-5

[3] Moore, J.H., Davis, C.C., Coplan M.A. and Greer, S.C. (2009) Building Scientific Apparatus. 4th Edition, Camdridge University Press, New York, 629 p. https://doi.org/10.1017/CBO9780511609794

[4] Imhof, R.E. and Read, F.H. (1968) A Three-Aperture Electron Optical Lens for Producing an Image of Variable Energy But Fixed Position. *Journal of Physics E*, **1**, 859-860. https://doi.org/10.1088/0022-3735/1/8/325

[5] Lee, S.Y. (2004) Accelerator Physics. 2nd Edition, World Scientific Publishing Co. Pte. Ltd, Singapore, 575 p. https://doi.org/10.1142/5761

[6] Toivanen, V., Kalvas, T., Koivisto, H., Komppula, J. and Tarvainen, O. (2013) Double Einzel Lens Extraction for the JYFL 14GHzECR Ion Source Designed with IBSimu. *Journal of Instrumentation*, **8**, 1-19. https://doi.org/10.1088/1748-0221/8/05/P05003

[7] Heddle, D.W.O. (2000) Electrostatic Lens Systems. 2nd Edition, IOP, London, 127 p. https://doi.org/10.1201/NOE0750306973

[8] Syms, R.R.A., Michelutti, L. and Ahmad, M.M. (2003) Two-Dimensional Microfabricated Electrostatic Einzel Lens. *Sensors and Actuators A*, **107**, 285-295. https://doi.org/10.1016/j.sna.2003.08.001

[9] Reiser, M. (2008) Theory and Design of Charged Particle Beams. Wiley-Vclt, Weinhein.

[10] Read, F.H. (1969) Calculated Properties of Electrostatic Einzel Lenses of Three Apertures. *Journal of Physics E*, **2**, 679-684. https://doi.org/10.1088/0022-3735/2/8/320

[11] Szilagyi (1987) Electrostatic Spline Lenses. *Journal of Vacuum Science & Technology A*: *Vacuum*, *Surfaces*, *and Films*, **5**, 273-278. https://doi.org/10.1116/1.574117

[12] Szilagyi, M. (1988) Electron and Ion Optics. 5th Edition, Plenum Press, New York, 539 p. https://doi.org/10.1007/978-1-4613-0923-9

[13] Lanczos, C. (2013) Applied Analysis. Dover Publications, New York.

[14] Szilagyi, M. (1986) Relativistic Trajectory Equations for Charged Particle S in General Orthogonal Curvilinear Coordinates. *Applied Physics Letters*, **49**, 740-742. https://doi.org/10.1063/1.97533

[15] Read, F.H. (1969) Accurate Calculations of Double-Aperture Electrostatic Immersion Lenses. *Journal of Physics E*, **2**, 165-169. https://doi.org/10.1088/0022-3735/2/2/311

[16] Leveneur, J. and Markwitz, A. (2008) Introduction to Simion 7. GNS 1, 23 p.

[17] Read, F.H., Adams, A. and Soto-Montiel, J.R. (1971) Electrostatic Cylinder Lenses: Two Element Lenses. *Journal of Physics E*, **4**, 625-632. https://doi.org/10.1088/0022-3735/4/9/001